Advancing surgical guidance: from (hybrid) molecule to man and beyond

Berg, N.S. van den

CHAPTER 3

HYBRID TRACERS FOR SENTINEL NODE BIOPSY

Adapted from: van den Berg NS, Buckle T, KleinJan GH, Klop WMC, Horenblas S, van der Poel HG, Valdés Olmos RA, van Leeuwen FWB. Q J Nucl Med Mol Imaging. 2014;58:193-206.

ABSTRACT

Conventional sentinel node (SN) mapping is performed by injection of a radiocolloid followed by lymphoscintigraphy to identify the number and location of the primary tumor draining lymph node(s), the so-called SN(s). Over the last decade research has focused on the introduction of new imaging agents that can further aid (surgical) SN identification. Different tracers for SN mapping, with varying sizes and isotopes have been reported, most of which have proven their value in a clinical setting. A major challenge lies in transferring this diagnostic information obtained at the nuclear medicine department to the operating theatre thereby providing the surgeon with (image) guidance. Conventionally, an intraoperative injection of vital blue dye or a fluorescence dye is given to allow intraoperative optical SN identification. However, for some indications, the radiotracer-based approach remains crucial. More recently, hybrid tracers, that contain both a radioactive and fluorescent label, were introduced to allow for direct integration of pre- and intraoperative guidance technologies. Their potential is especially high when they are used in combination with new surgical imaging modalities and navigation tools. Next to a description of the known tracers for SN mapping, this review discusses the application of hybrid tracers during SN biopsy and how the introduction of these new techniques can further aid in translation of nuclear medicine information into the operating theatre.

INTRODUCTION

The presence of metastases in the regional lymph node(s) is one of the most important prognostic factors in breast cancer and melanoma, but also in head-and-neck malignancies and cancers of the genitals. For example, in patients with head-and-neck malignancies it was shown that unilateral lymph node metastasis lowered the five-year survival rate with 50% [1].

A regional lymph node dissection can be performed to determine the lymph node status. Unfortunately this procedure is associated with high morbidity such as lymphedema. Assuming the orderly spread of tumor cells through the lymphatic system, identifying the primary tumor draining lymph node(s), the so-called sentinel node(s) (SN(s)) [2], will allow more accurate determination of the lymph node status in patients presenting without clinical evidence of regional lymph node involvement or distant metastasis (clinically N0M0). With roughly 10-30% of these patients presenting with occult lymph node metastases [3-5], SN biopsy can be used to stage these clinically N0 patients and select patients with positive SNs for a regional lymph node dissection as such sparing the pathologically N0 patients an unnecessary regional lymph node dissection. Moreover, with SN biopsy the accuracy of pathological lymph node staging will increase; the pathologist can meticulously examine the SNs only for the presence of isolated tumor cells and/or (micro-)metastases, which is not possible if he/she has to examine a whole regional lymph node dissection specimen (generally >20 lymph nodes).

SN biopsy is most widely validated and implemented in staging patients with breast cancer [6] and melanoma [7]. Over the last decade, SN biopsy has also found its way in staging the regional lymph nodes of the groin in patients with penile [8] or vulvar [9] cancer and for staging the neck in patients with head-and-neck squamous cell carcinoma [10]. The concept has also been validated for prostate cancer in various European countries [11-13], but the procedure has not yet been widely accepted. Initial work is also reported for other urological malignancies like testis [14,15], bladder [16], and kidney [17,18] cancer, as well as SN biopsy for lung [19] and gastric [20] cancer. The potential of lymph node mapping for colorectal cancer has been underlined by ex vivo SN mapping studies [21,22]. Expansion of the SN biopsy technique to these new indications will not only lead to an enlargement of the patient population that will undergo SN biopsy, the widespread implementation of this minimally invasive procedure will also increase the surgical complexity. For example, the surgeon's senses are reduced during laparoscopic applications, driving the need for innovations that aid the surgical identification.

Over the recent years, conventional SN mapping based on lymphoscintigraphy after injection of a radiotracer has been improved by the introduction of single photon emission computed tomography combined with computed tomography (SPECT/CT). Acquisition of SPECT scans enables visualization of the radioactive hot spots (SNs), and fusion of these images with CT images enables anatomical localization of the SN(s) [23,24]. Such an anatomical roadmap can be used to preoperatively plan the most optimal surgical approach towards the SN(s).

Generally, surgical identification of the preoperatively defined SNs can be performed using a gamma-ray detection probe (hereafter referred to as gamma probe) or a portable gamma camera that traces the radioactivity in the nodes, and/or by visual identification after an additional intraoperative injection of a vital blue dye. Unfortunately, in areas where SNs are often located near the injection site, e.g. head-and-neck cancers, radioactivity-based surgical identification can be difficult due to the high background signal coming from the injection site [25,26]. On the other hand, due to its passive diffusion through the lymphatic system, blue dye is unable to accumulate in the SN limiting its effective time window (30-45 minutes) [27]. In contrast, radiotracers are actively incorporated into SNs and can be detected >24 h after administration.

Ideally, the combined use of radiotracing and optical detection allows for optimal use of the nuclear and optical detection technologies. Herein radiotracing is most optimal for (preoperative) total body imaging and the identification of unexpected drainage patterns. Optical imaging, on the other hand, provides detail and real-time feedback during the surgical procedure regarding the location of the SN. Consequently the combination of the vital blue dye approach with radiotracing has been shown to yield a superior SN detection rate compared to either radiotracing or optical vital blue dye detection alone. For melanoma and breast cancer a success rate of identifying nodes with vital blue dye was shown to be 75-80% vs. 97-98% for radiocolloid-based SN detection [28,29]. This increased to 98-99% when using the combined approach of sequential injections. Yet for some indications, e.g. oral cavity carcinoma or prostate cancer, vital blue dye is less sensitive in the identification of the SNs than the radiocolloid approach, principally for the identification of aberrant drainage patterns as was shown in breast cancer where only 55% of SNs outside the axilla had stained blue vs. 84% of the axillary SNs [30]. Moreover, in oral cavity carcinoma and prostate cancer, vital blue dye administration was shown to be of limited value and/or to interfere with the visibility of tumor margins [3, 31, 32].

The limited sensitivity of vital blue dye detection was one of the main reasons to introduce (near-infrared) fluorescence tracers [33], and in particular indocyanine green (ICG) for SN biopsy. Fluorescent dyes show a comparable drainage pattern to vital blue dyes and as such they rapidly flow through the lymphatic system, without accumulation in the SNs [34]. In contrast to vital blue dyes, near-infrared dyes are invisible to the naked eye and can only be visualized using a dedicated near-infrared fluorescence camera system [35]. As such, the use of this type of dye does not interfere with margin visibility or unwanted coloring of the skin.

The difference in migration between the radiocolloid and the dyes can result in a discrepancy between the nuclear techniques used to non-invasively identify the SNs in the pre-surgical setting and the optical techniques used during surgery [28,29]. Direct integration of pre- and intraoperative imaging can be achieved by using hybrid tracers that contain both a radioactive and a fluorescent label [36,37].

This review gives an overview of the available lymphographic agents that are currently

clinically used for SN identification. Next, the application of hybrid tracers in the clinical routine and translation of nuclear medicine information into the operating theatre is discussed.

LYMPHOGRAPHIC AGENTS

RADIOTRACERS

For radiotracing in general colloid-based particles, ranging from albumin to tin, sulfur, antimony-trisulfide, rhenium and phytate are used (Figure 1). Following injection, these technetium-99m (^{99m}Tc) labeled colloids become trapped in the SN via an active physiological process in which the radiotracer is accumulated by macrophages and tissue histiocytes lining the sinuses of the node [38]. Ideally the agent should accumulate in the SN(s) with no, or limited, flow to higher-echelon nodes. However, when the flow is abundant and an excess of particles reaches the SN, saturation can occur, which in turn leads to overflow into higher-echelon nodes.

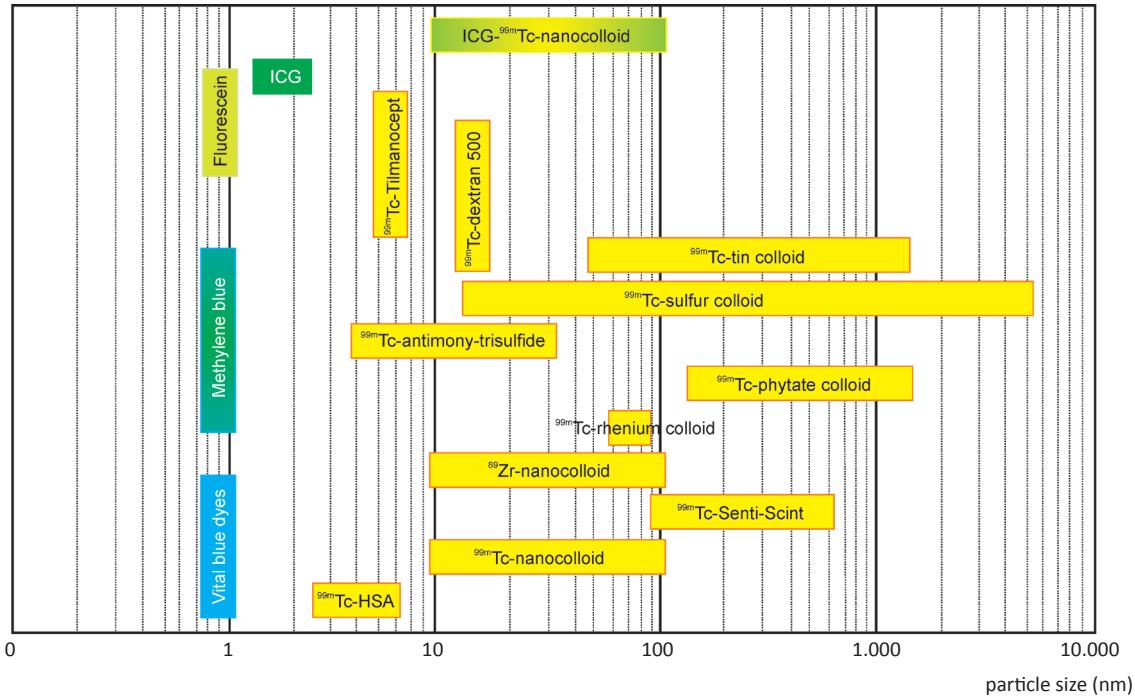

Figure 1. Overview of the particle sizes of the clinically available lymphographic agents. Vital blue dyes = indigo carmine, patent blue (V), isosulfan blue, and lymphazurin blue. ICG = indocyanine green; HSA = human serum albumin; Tc = technetium; Zr = zirkonium.

The composition and size of the current clinically used colloids varies greatly. Particles larger than 500 nm were shown to limit migration from the injection site [39], whereas smaller particles were reported to penetrate the capillary membranes, and as such might be unable to migrate through the lymphatic channel [40]. “Small-particle” radiocolloids (<100 nm) are thought to best enter the lymphatic vessels allowing visualization of the lymphatic tracts during dynamic lymphoscintigraphy [38]. Mariani et al. reported the use of 100-200 nm sized radiocolloids as the best compromise for efficient lymphatic drainage and retention in the SN(s) [29].

For metallic ^{99m}Tc-tin colloid the size depends on the ratio between the ^{99m}Tc-solution and tin solution; sizes ranging 50-1500 nm have been reported [41]. In the United States, the inorganic (filtered) ^{99m}Tc-sulfur colloid is the most frequently used tracer for SN mapping. Sizes ranging 100-400 nm [41] and 15-5000 nm [29] have been reported depending on the type of cut-off filter used. ^{99m}Tc-phytate is formed via a reaction with extracellular calcium and therefore the size of ^{99m}Tc-phytate colloid (diameter ranging 150-1500 nm) strongly depends on the serum calcium concentration [41]. ^{99m}Tc-antimony-trisulfide is mainly used in Australia and Canada and with a size ranging from 3-30 nm it is one of the smallest colloids [29,41] used for SN mapping. In Europe, human serum albumin (HSA)-based nanocolloids (mean diameter 20 nm; range 10-100 nm) are most widely used. Retention of this colloid in the SN is superior compared to that of radiolabeled HSA particles (mean diameter 7 nm) [34]. More recently, the larger HSA-based colloid Senti-Scint was introduced (mean diameter 205 nm; range 100-600 nm) and shown to allow for SN biopsy in amongst others breast [42] and prostate [13] cancer. This increase in size is thought to improve retention in the SNs but with lesser flow to higher-echelon nodes.

Alternatively, dextran-based particles (e.g. ^{99m}Tc-dextran 500 particles; approximately 14.4 nm [43]) have been used for lymphatic mapping in e.g. colon and breast cancer [44,45]. After many preclinical studies, a 7 nm radiocolloid based on mannose was evaluated in phase III studies for SN mapping in breast cancer, melanoma and squamous cell carcinoma of the oral cavity [46-48]. This tracer, better known as ^{99m}Tc-Tilmanocept or Lymphoseek™, is said to accumulate in SNs after binding the mannose-binding protein receptor present on phagocytes [49]. In contrast to the larger radiocolloids, these 7 nm particles also rapidly clear from the injection site due to diffusion into the blood capillaries leading to tracer absorption in the blood stream [49]. Although this diffusion may limit the amount of lymphatic flow, this clearance via the bloodstream reduces the signal intensity at the injection site, which may enable better identification of SN(s) located near the injection site.

As a substitute for the ^{99m}Tc-based radiotracers, zirkonium-89 (^{89}Zr) labeled nanocolloid (^{89}Zr-nanocolloid) has been introduced for positron emission tomography (PET)-based SN mapping in oral cavity carcinoma [50]. Compared to conventional lymphoscintigraphy and SPECT imaging, it is presumed that the increased sensitivity and resolution of PET imaging, in combination with CT, or possibly even magnetic resonance (MR) imaging, might be an

alternative for the ^{99m}Tc-based approach. Similar to the small dextran-based colloid this might also allow for better preoperative detection of SN(s) located near the injection site [50]. However, surgical SN detection using PET tracers has not yet been well-documented. Limiting for the wide implementation of PET/CT or PET/MR, or even PET/CT/MR approaches during SN mapping are the costs associated with production of tracers and the availability of the tracer at the clinical site.

Overall, comparison studies between the different lymphoscintigraphic tracers are limited and mainly focus on the evaluation of different particle sizes (in an in vitro setting) [51,52]. Most SN mapping studies compare the radioguided approach with optical vital blue dye detection. As such it is, at the moment, difficult to state which of the above-mentioned radiocolloids is superior. That said, the current used radiocolloids have proven their value for preoperative SN mapping, suggesting all of them perform to the specific in-house standards required for high-end patient care.

VITAL BLUE DYES

Vital blue dyes can be optically detected by the surgeons' eye during the operation due to absorption of light in the visual wavelength. After intraoperative injection, such a dye allows the surgeon to meticulously track the blue lymphatic duct(s) running from the injection site. Afferent tracts running to the SN(s) can be distinguished from efferent tracts leading to higher-echelon nodes. Literature reports the use of various vital blue dyes such as indigo carmine [53], patent blue (V) [4,5,25,30,37,54-58], isosulfan blue [20,47,48], lymphazurin blue [42,59], and methylene blue [59] (Figure 1). These small dyes (mean diameter <<1 nm) migrate quickly through the lymphatic system, thereby staining the lymphatic tract(s) and the lymph node blue. Unfortunately this occurs without any form of active accumulation in the SNs. In contrast to the other vital blue dyes, methylene blue is thought to be actively taken up by (cancer) cells via targeting the mitochondrial membrane potential [60]. This suggests that cancer cells present in the lymph node(s) might actively take up methylene blue, hereby improving the detection of tumor containing SN(s).

FLUORESCENT TRACERS

Although the principle of their use is the same to that of vital blue dyes, fluorescent dyes can be detected with higher sensitivity. Excitation of a fluorescent dye leads to internal conversion resulting in the emission of photons of a different, longer, wavelength [61]. Every fluorescent dye has its own particular excitation and emission wavelength [35,62]. Fluorescent dyes emitting in the visual range (400-650 nm) can also be detected by eye, but generally detection is more sensitive when a dedicated fluorescence camera is used. Using dedicated band pass filters a light sensitive camera can be used to detect fluorescence signals (photons) in a manner similar to the way gamma-rays are detected. An example of fluorescence imaging in the visual range can be found in fluorescein imaging, which fluoresces in marker-pen-yellow. Clinically fluorescein is used for angiography of the eye

[63] and has been widely used as a fluorescent alternative for the conventional vital blue dyes for lymphatic mapping in e.g. non-small cell lung cancer and colorectal cancer [56,64]. However, the use of fluorescent dyes with an emission in the visible range remains limited to superficial applications, as the tissue penetration of such dyes very limited (mm range).

To improve detection of more deeply situated SNs the use of dyes that emit in the near-infrared range (750-100 nm) have been opted (tissue penetration <1 cm). The best-known example of a clinically applied near-infrared dye can be found in ICG. ICG has been used for vascular perfusion measurements and (lymph-)angiography [65,66]. Currently ICG is widely applied during SN biopsy procedures in, e.g. breast cancer, melanoma, and vulvar cancer [65,66].

Methylene blue can, alternatively to optical blue dye-based detection, also be used as a fluorescent dye. When used at very low concentrations, methylene blue emits in the far-red range (650-750 nm) and has been used for fluorescence-based ureter [67] and parathyroid gland [68] visualization. Logically the same concept can be applied during SN biopsy procedures [69].

Initially it was suggested that the superior signal penetration achieved with a near-infrared fluorescence dye might replace the need for the radiotracer. However, like the blue dyes, fluorescent dyes show a fast migration through the lymphatic system and do not accumulate in the SN. Furthermore, several studies showed that although fluorescence imaging allowed for intraoperative identification of the SN(s), the limited degree of tissue penetration did not allow accurate SN mapping prior to surgery.

HYBRID TRACERS

To take advantage of the excellent properties of radiotracers for preoperative SN mapping and the high detection sensitivity of (near-infrared) fluorescent dyes during the operation, recently hybrid tracers combining radioactivity and fluorescence in one tracer were introduced. A great number of preclinically evaluated tracers potentially suited for hybrid SN mapping have been summarized previously [36]. Although not approved for clinical use, some of these tracers show great potential. For instance, a study in mice showed the combined use of ^{99m}Tc-Tilmanocept labeled with the near-infrared fluorescence dye Cy7 [70]. Alternatively, fluoride-18 fluoxydeglucose (^{18}F-FDG) was shown to allow for SN mapping [71]. Next to β^+-emission, ^{18}F-FDG also emits Cerenkov signals which can be detected similar a fashion as fluorescence [71,72]. Iron-based nanoparticles can also be labeled with fluorescent dyes (and/or and even radiolabels) yielding an alternative class of hybrid SN tracers that are also suitable for MR imaging [73,74].

The hybrid tracer ICG-^{99m}Tc-nanocolloid is formed via non-covalent self-assembly of two well-known lymphatic tracers, namely ICG and ^{99m}Tc-nanocolloid. This self-assembly is driven by the interaction of the dye with e.g. fatty acid binding pockets on albumin. This interaction is not limited to nanocolloid alone, albumin-based colloids in general can be coupled to ICG in a similar manner [34,76]. Other studies have shown that that combining

ICG with the inorganic ^{99m}Tc-sulfur colloid was not feasible and yielded a significant decrease in signal intensity of the fluorescence dye [77]. Clinically, ICG-^{99m}Tc-nanocolloid has, to date, been the most widely used hybrid tracer for SN biopsy. After its introduction for SN biopsy of prostate cancer [75], its application in head-and-neck melanoma [25,37], oral cavity carcinoma [26], breast [57], penile [37], and vulvar [55] cancer was shown. In a recent comparison study it was shown that ICG-^{99m}Tc-nanocolloid shows a similar drainage pattern as its parental compound ^{99m}Tc-nanocolloid [37]. With this tracer it was shown that preoperative SN mapping could be combined with intraoperative radio- and fluorescence guidance to the SN via one single injection of tracer.

Iodization of the dye methylene blue resulted in the formation of iodine-125 (^{125}I)-methylene blue. This compound has been evaluated in a clinical setting during SN biopsy for breast cancer [78,79]. Here, ^{125}I-methylene blue was intraoperatively administrated either subareolarly or intratumorally allowing for radiotracing and optical blue dye detection of the intraoperatively identified SN.

Next to the above-mentioned radioactive and optical tracers for lymphatic mapping, X-ray contrast [80] and magnetic nanoparticles [81] have been opted. In addition to the development of tracers that aid the surgical identification of the SN as such to (histo-) pathologically determine the regional lymph node status, ongoing research focuses on developing a method to non-invasively determine the regional lymph node status. For example, ultrasmall supra-paramagnetic iron oxide particles have been proposed for lymphatic mapping. Here the obtained negative contrast is suspicious of the presence of lymph node metastasis [82]. (Tumor-targeted) PET tracers might also be used for the detection of lymph node metastasis. Contrast-enhanced ultrasound and the injection of microbubbles have also been proposed for SN mapping [83]. From a preclinical point of view, targeted dendrimers, liposomes and even viral particles have been proposed for (tumor-targeted) lymph node mapping [84].

HYBRID TRACERS IN CLINICAL LOGISTICS

Implementation of hybrid tracers into the clinical routine has been shown to be feasible [37]. In case of ICG-^{99m}Tc-nanocolloid tracer preparation is slightly altered compared to the use of radiocolloid only. ICG is added to the radiocolloid solution, which is then almost immediately ready for administration [37]. Consequently use of these tracers does not lead to important alterations in the preparation procedure.

While the clinical advantages of combining preoperative and intraoperative imaging are clear, slight alterations in the workflow have to be made to incorporate both visualization methods simultaneously. Based on the clinical logistics, in the following section, we discuss the challenges and additional possibilities that arise during different steps in the clinical process when using a hybrid tracer (Figure 2).

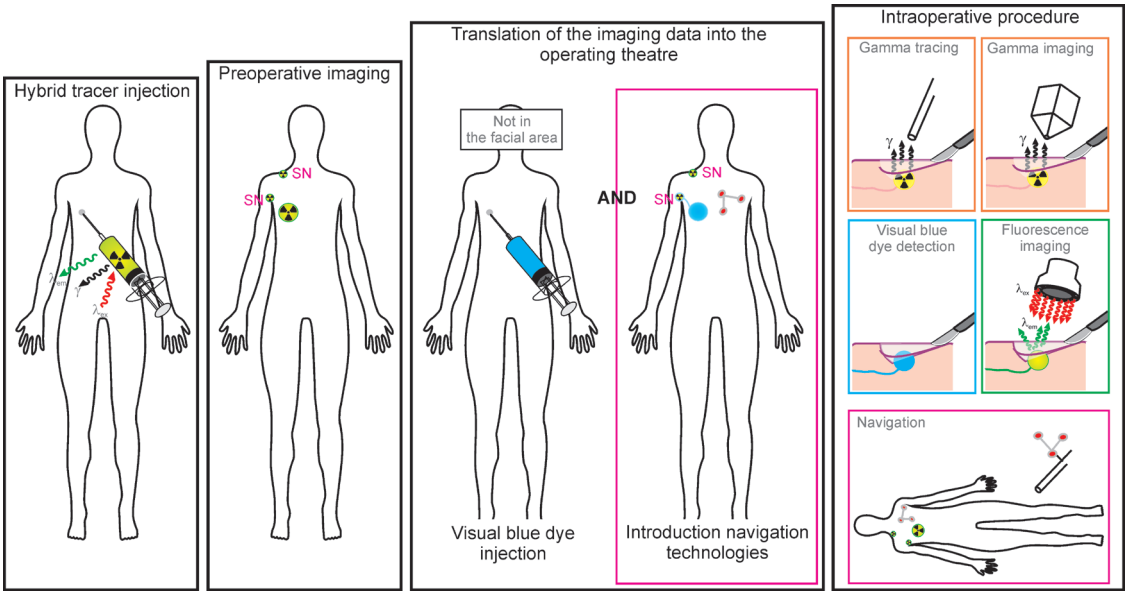

Figure 2. Schematic overview the concept of the use of hybrid tracers in a clinical setting. Following the injection of a hybrid tracer, preoperative lymphoscintigraphy and SPECT/CT imaging is performed to determine the number and anatomical location of the SN(s). An intraoperative injection with blue dye is given to allow for optical SN identification. Additionally, to improve the translation of preoperatively acquired imaging data into the operating theatre, navigation technologies can be introduced. Intraoperatively, a combination of gamma tracing, gamma imaging and fluorescence imaging and blue dye detection is used to identify the SNs. With the introduction of navigation technologies into the operating theatre, navigation of e.g. the gamma probe in the acquired SPECT images can allow for navigation-based identification of the SN(s). λem = emission wavelength of the fluorophore; λex = excitation wavelength of the fluorophore; γ = gamma signal coming from the radioisotope ICG = indocyanine green; SN = sentinel node.

TRACER INJECTION

In line with the SN concept, tracer administration must be related to the site of the tumor. Since the drainage pattern of the various lymphoscintigraphic tracers is dictated by the lymphatic anatomy present at the injection site, the location of tracer deposition is of great influence on the observed drainage pattern and the identification of the SN(s). Multiple injections are administrated around the tumor or excision scar in melanoma or cancer of the genitalia. For breast cancer, there is somewhat of a controversy and injection strategies may differ. Some prefer tumor-related (peritumoral or intratumoral) injections, whereas others prefer injections related to the skin (subdermal or intradermal) or aureolar (subaureolar or periaureolar). The concept here is that a periaureolar or other superficial injections will mainly help visualize only axillary lymphatic drainage [85]. In contrast, an intra- or peritumoral injection not only leads to axillary lymphatic drainage, but often

results in the visualization of drainage outside the axilla to locations such as the intramammary, periscapular or even parasternal regions. Hence, the periaureolar tracer administration approach may not accurately represent the drainage pattern of the tumor. A recent Multisent study, in patients with multifocal and multicentric breast cancer, underlined that each individual breast tumor can have its own specific drainage pattern [54]. Following the identification of the SNs draining from the largest tumor in the breast, additional drainage from the second or third injected tumor was identified in 64% of patients. In 56% of these patients, SNs found after this second/third injection were localized in different basins than those identified after the first injection. In two patients, isolated tumor cells were found in SNs that were only visualized after the second tumor had been injected [54]. For this study, the second/third injection was given 4-26 h after the injection in the largest tumor as such allowing for preoperative discrimination of the SNs from the different tumors. To improve these logistics, here hybrid tracers, in combination with the conventional radiocolloids can possibly be used to assess these multifocal and multicentric tumors via an injection protocol in which the different tumors are injected simultaneously with either the radiocolloid (largest tumor) or with the hybrid tracer (second/third tumor). The presence of fluorescence in the SNs during surgery can then be used to discriminate the different drainage pattern of these tumors.

When performing SN biopsy of e.g. for kidney or prostate cancer, but also for (non-palpable) breast cancer, tracer administration can be more challenging. For breast cancer, (non-palpable) tumors are generally injected under ultrasound or stereotaxic guidance. Tracer injections for abdominal tumors are generally performed under transrectal or endoscopic ultrasound guidance. Commonly an intratumoral injection, or an injection in the area most likely to contain tumor, is aimed for. Limiting in the injection accuracy is the availability of tumor specific needle navigation technologies.

The use of a hybrid tracer does not affect the manner of tracer injection. Like radiotracers, hybrid tracers can be used to assess the accuracy of tracer injection using the radioactive signature. By placing a handheld or portable gamma camera over the site of injection, deposition of the tracer can be checked for [75], and possible leakage into the bloodstream or bladder can be evaluated.

Where the radioactive component of hybrid tracers can be used during pre- and intraoperative imaging, the fluorescent component can also be exploited during ex vivo evaluation of the excised tissue [26, 86]. Not only can the distribution of the tracer in the SN be evaluated, assessment of the relation between the injection site and the corresponding drainage pattern can be used to improve the injection procedure. Assessment of the correlation between the location of the tracer deposits in excised prostate samples and the number and location of the preoperatively visualized SNs suggested that the location at which the tracer is deposited influences the lymphatic drainage pattern [86]. As such we reason that a more tumor directed tracer administration will likely result in improved identification of the true tumor draining lymph node(s) for that specific type of cancer.

PREOPERATIVE SENTINEL NODE MAPPING

Preoperatively, hybrid tracers can be used in an identical manner as the conventional radiotracers are used. Preoperative SN mapping is generally performed by acquisition of dynamic lymphoscintigrams immediately after tracer injection followed by static anterior, lateral and/or posterior lymphoscintigrams. Combined evaluation of these images allows identification of the SN(s) and higher-echelon nodes. With the introduction of SPECT/CT localization of these hot spots within their anatomical context became feasible [24]. This supplementary three-dimensional (3D) information allows the surgeon to plan his/her approach before the start of the operation. SPECT/CT imaging was found to be of particular value for the identification of SNs localized in areas with a complex anatomy and close to the injection site. Moreover, with SPECT/CT being more sensitive that conventional lymphoscintigraphy, non-visualization on planar lymphoscintigraphy can yield a SN when performing SPECT/CT imaging [58]. Additionally, SPECT/CT allows the identification of additional SNs not seen on lymphoscintigrams [58].

The improved resolution and sensitivity of PET/CT may provide a valuable alternative for SPECT/CT, and may allow for more clear identification of SNs located near the injection site [50]. However, a full dynamic procedure that also allows the identification of the lymphatic tract(s) running to the SN is, similar to lymphoscintigraphy, is still lacking for PET tracers.

The use of a handheld or portable gamma cameras can also be used for preoperative SN mapping. With their improved resolution compared that of conventional lymphoscintigraphy, and the ability to position the gamma camera closely to the skin of the patient, this might allow for the identification of near-injection site SNs [87] (an overview of available handheld and portable gamma cameras is given in [88]).

INTRAOPERATIVE IMAGING AND TRANSLATION OF PREOPERATIVE IMAGING INTO THE OPERATING THEATRE

Conform the standard procedure, projection of the data generated at nuclear medicine in the operating theatre, either on-screen [25,26,37,55,75], on an iPad [89] or loading these data into the da Vinci robot during robot-assisted laparoscopic procedures [90,91] can provide the surgeons with feedback regarding the location of the SN during the operation. The most simple way to guide a surgeon to the radioactive hot spots in the patient is probably gamma tracing using a collimator-based gamma probe. The introduction of portable gamma camera technologies into the operating theatre provided surgeons with the ability to generate a pre-incision image of the location of the radioactive hot spots. In a similar fashion this approach was also found to be of value to confirm the removal of the SNs. For example, in six patients with head-and-neck malignancies, with the portable gamma camera nine additional SNs were identified in the wound area after the initial SN had been excised. One of these additionally excised SNs was found to be tumor-positive [92].

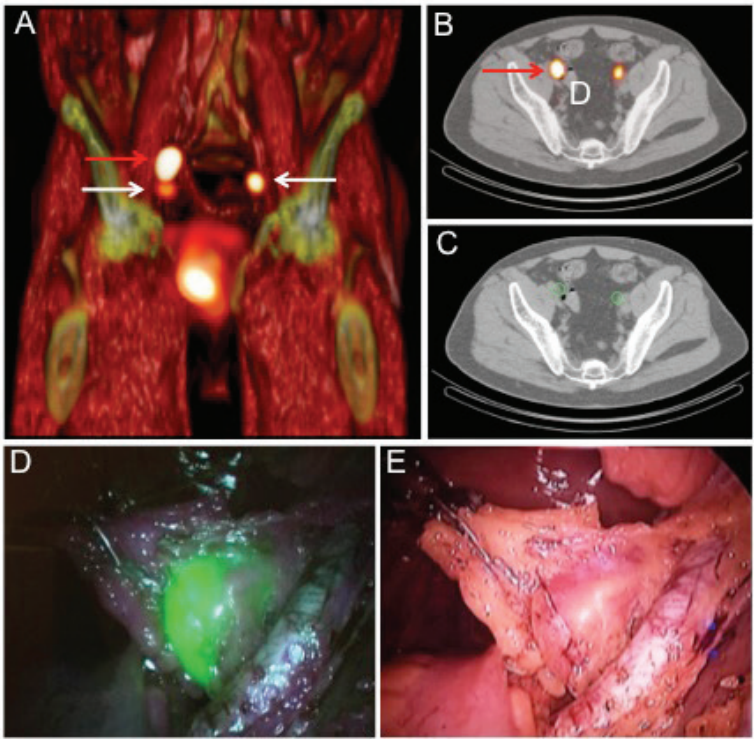

Figure 3. Implementation of the hybrid tracer during robot-assisted laparoscopic sentinel node biopsy of prostate cancer. A) 3D volume rendering of fused SPECT and CT images showing three SNs (arrows); B) axial fused SPECT and CT image showing the location of the most right cranial hot spot in the external iliac area (red arrow). C) Corresponding CT slide; D) Fluorescence imaging of the right most cranial SN using the fluorescence laparoscope from KARL STORZ Endoskope GmbH & Co. KG (Image 1 HUB HD); E) Corresponding white light image of the SN. 3D = three-dimentional; SPECT = single photon emission computed tomography; CT = computed tomography; SN = sentinel node.

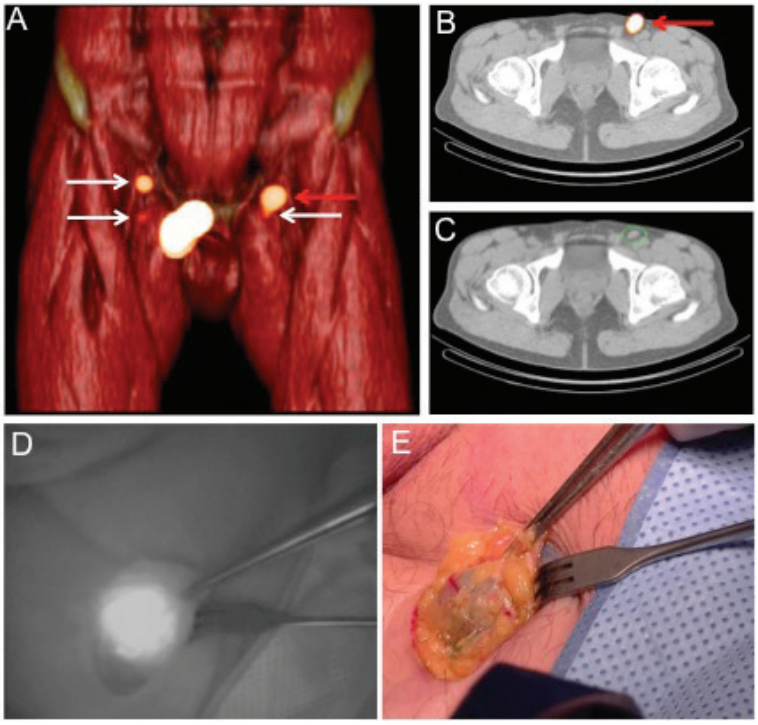

Figure 4. Implementation of the hybrid tracer during SN biopsy for penile cancer. A) 3D volume rendering of fused SPECT and CT images showing 4 of the 5 preoperatively defined SNs (arrows); B) Axial fused SPECT and CT image showing the location of the most left cranial hot spot in the inguinal zone (red arrow); C) Corresponding CT slide; D) Fluorescence imaging of the right most cranial SN using the handheld fluorescence camera from Hamamatsu Photonics K.K. (PhotoDynamic Eye); E) Corresponding white light image of the SN. This SN was found to be slightly blue. 3D = three-dimentional; SPECT = single photon emission computed tomography; CT = computed tomography; SN = sentinel node.

Radioguidance might be hampered with an increased time between injection and the start of surgery, or with SNs being located near the injection site due to signal bleeding. Hybrid tracers such as ICG-^{99m}Tc-nanocolloid enable intraoperative surgical visualization of the preoperatively identified SNs using a dedicated near-infrared fluorescence camera (Figures 3, 4). With the fluorescence signal remaining stable over time, providing its not being exposed to an excess of light, and the limited penetration depth of the fluorescence signal in comparison to that of the radioactive signal, the fluorescence signature of the hybrid tracer can overcome these hurdles. Especially in areas where no vital blue dye is used, in areas with a complex anatomy or in areas with near-injection site SNs, the value of fluorescence imaging was found to be prominent [25,26,75]. In addition, the SN identification rate via the fluorescent signature of the hybrid tracer was found to be superior to that achieved with vital blue dye alone. For example, in vulvar carcinoma intraoperatively 96% of SNs could be visualized with fluorescence imaging whereas only 65% of these nodes were stained blue [55].

Obviously, the implementation of additional visualization methods into the clinical routine affects the surgical workflow. Depending on the type of (handheld) fluorescence camera used in open surgical procedures, the light in the operating theatre needs to be dimmed when fluorescence imaging is initiated to allow for better contrast between the signal in the SN and the background; the light used in the operating theatre contain a fair amount of near-infrared light and the intensity of this light will prohibit the identification of the SN via fluorescence imaging. During laparoscopic procedures, this is not a requirement. This feature is not related to the use of hybrid imaging agents, but to intraoperative fluorescence imaging in general. Improvements of currently available (laparoscopic) camera systems might partially overcome this [35].

In our experience implementation of an additional imaging modality, such as an fluorescence camera, can lead to improved intraoperative detection of the SN. After an initial adjustment period and proper training of surgeons and scrub-nurses, combined radiotracing and intraoperative fluorescence imaging can be fully adopted into the existing surgical routine.

FUTURE APPLICATIONS: INTRODUCTION OF NAVIGATION TECHNOLOGIES INTO THE CLINIC

The introduction of intraoperative navigation can further aid the translation of diagnostic (nuclear medicine-derived) information in the operating theatre. Very simple, for SN biopsy of prostate cancer, the use of a portable gamma camera in combination with real-time on-screen tracking of an ^{125}I-seed placed on a laparoscopic gamma probe was shown to result in two-dimensional navigation to SN(s) [93].

To further improve the intraoperative detection accuracy of the preoperatively defined SN(s), the concept of intraoperative freehandSPECT was introduced by Wendler et al. [94] and implemented firstly in the clinic in 2010 in patients with breast cancer [95]. With this approach, real-time scanning of an area of interest with a gamma probe enables the generation of an intraoperative 3D SPECT scan. Similar to portable gamma cameras, the generation of this intraoperative freehandSPECT scan allows planning of the excision of the SN(s) whereas post-excision scanning of the same area allows confirmation of removal of the SN(s). In addition, the surgeon can navigate the gamma probe, in augmented-reality, in this 3D SPECT scan to the lesion of interest thereby possibly "easing" its identification. Recently this approach was also shown to be feasible for oral cavity carcinoma [96] and melanoma [97].

More recently, navigation based on reference targets in combination with preoperatively acquired nuclear medicine or radiology data was shown [98]. The accuracy of this technology strongly depends on the accuracy with which the preoperative situation can be reproduced; organ movement or deformation due to e.g. patient position changes limit the accuracy [99,100]. These movements are difficult to correct for with internal or external navigation aids, as placement of these aids can also cause additional placement errors [99,100]. The combination of navigation with a real-time imaging technology, e.g. fluorescence imaging, that can determine the navigation accuracy helps the surgeon to correct for errors. In a recent study by Brouwer et al. the feasibility of this approach was shown using ICG-^{99m}Tc-nanocolloid [58]. During preoperative SPECT/CT imaging, a reference target was placed on the patient' body. Repositioning of a sterile reference target on the exact same location on the patient' body in the operating theater allowed a mixed-reality integration of the preoperatively acquired SPECT/CT scan and a visual image of the patient lying on the operating table. Tracking of the fluorescence laparoscope (Image 1 HUB HD; KARL STORZ Endoskope GmbH & Co. KG, Tuttlingen, Germany) allowed reality 3D SPECT/CT-based navigation of this surgical tool. With decreasing distance towards the prostate, the fluorescence signal increased. Hence fluorescence imaging could be used to compensate for errors created due to patient positioning [98].

CONCLUSION

There lies great promise in combining lymphoscintigraphic agents and fluorescent agents for SN mapping. The introduction of hybrid tracers, in which fluorescence dyes and radiotracers are combined, allows for both intraoperative radio- and fluorescence guidance to the SN via one single injection of tracer whereas the protocol of preoperative SN mapping using lymphoscintigraphy and SPECT/CT imaging remains unmodified. The incorporation of fluorescence imaging into the daily used radioguidance technologies opens a whole new line of research.

REFERENCES

1. Ahuja AT, Ying M, Ho SY, Antonio G, Lee YP, King AD et al. Ultrasound of malignant cervical lymph node (s). Cancer Imaging. 2008;8:48-56.
2. Nieweg OE, Tanis PJ, Kroon BB. The definition of a sentinel node. Ann Surg Oncol. 2001;8:538-41.
3. Broglie MA, Stoeckli SJ. Relevance of sentinel node procedures in head and neck squamous cell carcinoma. Q J Nucl Med Mol Imaging. 2011;55:509-20.
4. Horenblas S, Jansen L, Meinhardt W, Hoefnagel CA, de Jong D, Nieweg OE. Detection of occult metastasis in squamous cell carcinoma of the penis using a dynamic sentinel node procedure. J Urol. 2000;163:100-4.
5. Van der Zee AG, Oonk MH, De Hullu JA, Ansink AC, Vergote I, Verheijen RH et al. Sentinel node dissection is safe in the treatment of early-stage vulvar cancer. J Clin Oncol. 2008;26:884-9.
6. Lyman GH, Giuliano AE, Somerfield MR, Benson AB, 3rd, Bodurka DC, Burstein HJ et al. American Society of Clinical Oncology guideline recommendations for sentinel lymph node biopsy in early-stage breast cancer. J Clin Oncol. 2005;23:7703-20.
7. Morton DL, Thompson JF, Cochran AJ, Mozzillo N, Elashoff R, Essner R et al. Sentinel-node biopsy or nodal observation in melanoma. New Engl J Med. 2006;355:1307-17.
8. Sadeghi R, Gholami H, Zakavi SR, Kakhki VR, Tabasi KT, Horenblas S. Accuracy of sentinel lymph node biopsy for inguinal lymph node staging of penile squamous cell carcinoma: systematic review and meta-analysis of the literature. J Urol. 2012;187:25-31.
9. Hassanzade M, Attaran M, Treglia G, Yousefi Z, Sadeghi R. Lymphatic mapping and sentinel node biopsy in squamous cell carcinoma of the vulva: systematic review and meta-analysis of the literature. Gynecol Oncol. 2013;130:237-45.
10. Alkureishi LW, Ross GL, Shoaib T, Soutar DS, Robertson AG, Thompson R et al. Sentinel node biopsy in head and neck squamous cell cancer: 5-year follow-up of a European multicenter trial. Ann Surg Oncol. 2010;17:2459-64.
11. Meinhardt W, van der Poel HG, Valdes Olmos RA, Bex A, Brouwer OR, Horenblas S. Laparoscopic sentinel lymph node biopsy for prostate cancer: the relevance of locations outside the extended dissection area. Prostate Cancer. 2012;2012:751-3.
12. Rousseau C, Rousseau T, Bridji B, Pallardy A, Lacoste J, Campion L et al. Laparoscopic sentinel lymph node (SLN) versus extensive pelvic dissection for clinically localized prostate carcinoma. Eur J Nucl Med Mol Imaging. 2012;39:291-9.
13. Jeschke S, Beri A, Grull M, Ziegerhofer J, Prammer P, Leeb K et al. Laparoscopic radioisotope-guided sentinel lymph node dissection in staging of prostate cancer. Eur Urol. 2008;53:126-32.
14. Brouwer OR, Valdes Olmos RA, Vermeeren L, Hoefnagel CA, Nieweg OE, Horenblas S. SPECT/CT and a portable gamma-camera for image-guided laparoscopic sentinel node biopsy in testicular cancer. J Nucl Med. 2011;52:551-4.
15. Tanis PJ, Horenblas S, Valdes Olmos RA, Hoefnagel CA, Nieweg OE. Feasibility of sentinel

node lymphoscintigraphy in stage I testicular cancer. Eur J Nucl Med Mol Imaging. 2002;29:670-3.
16. Liedberg F, Chebil G, Davidsson T, Gudjonsson S, Mansson W. Intraoperative sentinel node detection improves nodal staging in invasive bladder cancer. J Urol. 2006;175:84-8.
17. Bex A, Vermeeren L, Meinhardt W, Prevoo W, Horenblas S, Valdes Olmos RA. Intraoperative sentinel node identification and sampling in clinically node-negative renal cell carcinoma: initial experience in 20 patients. World J Urol. 2011;29:793-9.
18. Sherif AM, Eriksson E, Thorn M, Vasko J, Riklund K, Ohberg L et al. Sentinel node detection in renal cell carcinoma. A feasibility study for detection of tumour-draining lymph node (s). BJU Int. 2012;109:1134-9.
19. Nomori H, Kohno M, Izumi Y, Ohtsuka T, Asakura K, Nakayama T. Sentinel nodes in lung cancer: review of our 10-year experience. Surg Today. 2011;41:889-95.
20. Kitagawa Y, Takeuchi H, Takagi Y, Natsugoe S, Terashima M, Murakami N et al. Sentinel node mapping for gastric cancer: a prospective multicenter trial in Japan. J Clin Oncol. 2013; 31:3704-10.
21. van der Pas MH, Meijer S, Hoekstra OS, Riphagen II, de Vet HC, Knol DL et al. Sentinel-lymph-node procedure in colon and rectal cancer: a systematic review and meta-analysis. Lanet Oncol. 2011;12:540-50.
22. van der Zaag ES, Bouma WH, Tanis PJ, Ubbink DT, Bemelman WA, Buskens CJ. Systematic review of sentinel lymph node mapping procedure in colorectal cancer. Ann Surg Oncol. 2012;19:3449-59.
23. Mariani G, Bruselli L, Kuwert T, Kim EE, Flotats A, Israel O et al. A review on the clinical uses of SPECT/CT. Eur J Nucl Med Mol Imaging. 2010;37:1959-85.
24. Olmos RA, Vidal-Sicart S, Nieweg OE. SPECT-CT and real-time intraoperative imaging: new tools for sentinel node localization and radioguided surgery? Eur J Nucl Med Mol Imaging. 2009;36:1-5.
25. Brouwer OR, Klop WM, Buckle T, Vermeeren L, van den Brekel MW, Balm AJ et al. Feasibility of sentinel node biopsy in head and neck melanoma using a hybrid radioactive and fluorescent tracer. Ann Surg Oncol. 2012;19:1988-94.
26. van den Berg NS, Brouwer OR, Klop WM, Karakullukcu B, Zuur CL, Tan IB et al. Concomitant radio- and fluorescence-guided sentinel lymph node biopsy in squamous cell carcinoma of the oral cavity using ICG-(^{99m})Tc-nanocolloid. Eur J Nucl Med Mol Imaging. 2012;39:1128-36.
27. Rietbergen DD, van den Berg NS, van Leeuwen FW, Valdes Olmos R. Hybrid techniques for intraoperative sentinel lymph node imaging: early experiences and future prospects. Future Medicine. 2013;5:147-59.
28. Mariani G, Erba P, Manca G, Villa G, Gipponi M, Boni G et al. Radioguided sentinel lymph node biopsy in patients with malignant cutaneous melanoma: the nuclear medicine contribution. J Surg Oncol. 2004;85:141-51.
29. Mariani G, Erba P, Villa G, Gipponi M, Manca G, Boni G et al. Lymphoscintigraphic and

intraoperative detection of the sentinel lymph node in breast cancer patients: the nuclear medicine perspective. J Surg Oncol. 2004;85:112-22.
30. Jansen L, Doting MH, Rutgers EJ, de Vries J, Olmos RA, Nieweg OE. Clinical relevance of sentinel lymph node(s) outside the axilla in patients with breast cancer. Br J Surg. 2000;87:920-5.
31. Kuriakose MA, Trivedi NP. Sentinel node biopsy in head and neck squamous cell carcinoma. Curr Opin Otolaryngol Head Neck Surg. 2009;17:100-10.
32. Egawa M, Fukuda M, Takashima H, Misaki T, Kinuya K, Terahata S. The sentinel node concept in prostate cancer: Present reality and future prospects. Indian J Urol. 2008;24:451-6.
33. Vahrmeijer AL, Frangioni JV. Seeing the invisible during surgery. Br J Surg. 2011;98:749-50.
34. van Leeuwen AC, Buckle T, Bendle G, Vermeeren L, Valdes Olmos R, van de Poel HG et al. Tracer-cocktail injections for combined pre- and intraoperative multimodal imaging of lymph node(s) in a spontaneous mouse prostate tumor model. J Biomed Opt. 2011;16:016004.
35. van den Berg NS, van Leeuwen FW, van der Poel HG. Fluorescence guidance in urologic surgery. Curr Opin Urol. 2012;22:109-20.
36. Buckle T, Chin PT, van Leeuwen FW. (Non-targeted) radioactive/fluorescent nanoparticles and their potential in combined pre- and intraoperative imaging during sentinel lymph node resection. Nanotechnology. 2010;21:482001.
37. Brouwer OR, Buckle T, Vermeeren L, Klop WM, Balm AJ, van der Poel HG et al. Comparing the hybrid fluorescent-radioactive tracer indocyanine green-^{99m}Tc-nanocolloid with ^{99m}Tc-nanocolloid for sentinel node identification: a validation study using lymphoscintigraphy and SPECT/CT. J Nucl Med. 2012;53:1034-40.
38. Uren RF. Lymphatic drainage of the skin. Ann Surg Oncol. 2004;11:179S-85S.
39. Ege GN. Internal mammary lymphoscintigraphy. The rationale, technique, interpretation and clinical application: a review based on 848 cases. Radiology. 1976;118:101-7.
40. Henze E, Schelbert HR, Collins JD, Najafi A, Barrio JR, Bennett LR. Lymphoscintigraphy with Tc-99m-labeled dextran. J Nucl Med. 1982;23:923-9.
41. Higashi H, Natsugoe S, Uenosono Y, Ehi K, Arigami T, Nakabeppu Y et al. Particle size of tin and phytate colloid in sentinel node identification. J Surg Research. 2004;121:1-4.
42. Mirzaei S, Rodrigues M, Hoffmann B, Knoll P, Riegler-Keil M, Kreuzer W et al. Sentinel lymph node detection with large human serum albumin colloid particles in breast cancer. Eur J Nucl Med Mol Imaging. 2003;30:874-8.
43. Li S, Nguyen L, Xion H, Wang M, Hu TC-C, She J-X et al. Nanocarriers for biomedical applications. J S C Aca Sci. 2011;9:30-2.
44. Reasbeck PG, Manktelow A, McArthur AM, Packer SG, Berkeley BB. An evaluation of pelvic lymphoscintigraphy in the staging of colorectal carcinoma. Br J Surg. 1984;71:936-40.
45. Xavier NL, Amaral BB, Cerski CT, Fuchs SC, Spiro BL, Oliveira OL et al. Sentinel lymph

node identification and sampling in women with early breast cancer using 99m-Tc labelled dextran 500 and patent blue V dye. Nucl Med Comm. 2001;22:1109-17.
46. Marcinow AM, Hall N, Byrum E, Teknos TN, Old MO, Agraw-al A. Use of a Novel Receptor-Targeted (CD206) Radiotracer, ^{99m}Tc-Tilmanocept, and SPECT/CT for Sentinel Lymph node Detection in Oral Cavity Squamous Cell Carcinoma: Initial Institutional Report in an Ongoing Phase 3 Study. JAMA Otolaryngol Head Neck Surg. 2013;139:895-902.
47. Sondak VK, King DW, Zager JS, Schneebaum S, Kim J, Leong SP et al. Combined analysis of phase III trials evaluating [(9)(9)mTc]tilmanocept and vital blue dye for identification of sentinel lymph node (s) in clinically node-negative cutaneous melanoma. Ann Surg Oncol. 2013;20:680-8.
48. Wallace AM, Han LK, Povoski SP, Deck K, Schneebaum S, Hall NC et al. Comparative evaluation of [(99m)tc] tilmanocept for sentinel lymph node mapping in breast cancer patients: results of two phase 3 trials. Ann Surg Oncol. 2013;20:2590-9.
49. Vera DR, Wallace AM, Hoh CK, Mattrey RF. A synthetic macromolecule for sentinel node detection: (99m)Tc-DTPA-mannosyl-dextran. J Nucl Med. 2001;42:951-9.
50. Heuveling DA, van Schie A, Vugts DJ, Hendrikse NH, Yaqub M, Hoekstra OS et al. Pilot study on the feasibility of PET/CT lymphoscintigraphy with 89Zr-nanocolloidal albumin for sentinel node identification in oral cancer patients. J Nucl Med. 2013;54:585-9.
51. Jankovic D, Maksin T, Djokic D, Milonjic S, Nikolic N, Mirkovic M et al. Particle size analysis: 90Y and ^{99m}Tc-labelled colloids. J Microsc. 2008;232:601-4.
52. Tsopelas C. Particle size analysis of (^{99m})Tc-labeled and unlabeled antimony trisulfide and rhenium sulfide colloids intended for lymphoscintigraphic application. J Nucl Med. 2001;42:460-6.
53. Uhara H, Yamazaki N, Takata M, Inoue Y, Sakakibara A, Nakamura Y et al. Applicability of radiocolloids, blue dyes and fluorescent indocyanine green to sentinel node biopsy in melanoma. J Dermatol. 2012;39:336-8.
54. Brouwer OR, Vermeeren L, van der Ploeg IM, Valdes Olmos RA, Loo CE, Pereira-Bouda LM et al. Lymphoscintigraphy and SPECT/CT in multicentric and multifocal breast cancer: does each tumour have a separate drainage pattern? Results of a Dutch multicentre study (MULTISENT). Eur J Nucl Med Mol Imaging. 2012;39:1137-43.
55. Matheron HM, van den Berg NS, Brouwer OR, Kleinjan GH, van Driel WJ, Trum JW et al. Multimodal surgical guidance towards the sentinel node in vulvar cancer. Gynecol Oncol. 2013;131:720-5.
56. Meyer A, Cheng C, Antonescu C, Pezzetta E, Bischof-Delaloye A, Ris HB. Successful migration of three tracers without identification of sentinel nodes during intraoperative lymphatic mapping for non-small cell lung cancer. Interact Cardiovasc Thorac Surg. 2007;6:214-8.
57. Schaafsma BE, Verbeek FP, Rietbergen DD, van der Hiel B, van der Vorst JR, Liefers GJ et al. Clinical trial of combined radio- and fluorescence-guided sentinel lymph node biopsy in breast cancer. Br J Surg. 2013;100:1037-44.

58. van der Ploeg IM, Valdes Olmos RA, Kroon BB, Nieweg OE. The Hybrid SPECT/CT as an additional lymphatic mapping tool in patients with breast cancer. World J Surg. 2008;32:1930-4.
59. Liu Y, Truini C, Ariyan S. A randomized study comparing the effectiveness of methylene blue dye with lymphazurin blue dye in sentinel lymph node biopsy for the treatment of cutaneous melanoma. Ann Surg Oncol. 2008;15:2412-7.
60. Eckert GP, Renner K, Eckert SH, Eckmann J, Hagl S, Abdel-Kader RM et al. Mitochondrial dysfunction a pharmacological target in Alzheimer's disease. Mol Neurobiol. 2012;46:136-50.
61. Ruggi A, van Leeuwen FW, Velders AH. Interaction of dioxygen with the electronic excited state of Ir(III) and Ru(II) complexes: Principles and biomedical applications. Coord Chem Rev. 2011;255:2542-54.
62. Yuan L, Lin W, Zheng K, He L, Huang W. Far-red to near infrared analyte-responsive fluorescent probes based on organic fluorophore platforms for fluorescence imaging. Chem Soc Rev. 2013;42:622-61.
63. Spaide RF. Peripheral areas of nonperfusion in treated central retinal vein occlusion as imaged by wide-field fluorescein angiography. Retina. 2011;31:829-37.
64. Dan AG, Saha S, Monson KM, Wiese D, Schochet E, Barber KR et al. 1% lymphazurin vs. 10% fluorescein for sentinel node mapping in colorectal tumors. Arch Surg. 2004;139:1180-4.
65. Polom K, Murawa D, Rho YS, Nowaczyk P, Hunerbein M, M rawa P. Current trends and emerging future of indocyanine green usage in surgery and oncology: a literature review. Cancer. 2011;117:4812-22.
66. Schaafsma BE, Mieog JS, Hutteman M, van der Vorst JR, Kuppen PJ, Lowik CW et al. The clinical use of indocyanine green as a near-infrared fluorescent contrast agent for image-guided oncologic surgery. J Surg Oncol. 2011;104:323-32.
67. Verbeek FP, van der Vorst JR, Schaafsma BE, Swijnenburg RJ, Gaarenstroom KN, Elzevier HW et al. Intraoperative near infrared fluorescence guided identification of the ureters using low dose methylene blue: a first in human experience. J Urol. 2013;190:574-9.
68. van der Vorst JR, Schaafsma BE, Verbeek FP, Swijnenburg RJ, Tummers Q, Hutteman M et al. Intraoperative near-infrared fluorescence imaging of parathyroid adenomas using low-dose methylene blue. Head Neck. 2014;36:853-8.
69. Chu M, Wan Y. Sentinel lymph node mapping using near-infrared fluorescent methylene blue. J Biosci Bioeng. 2009;107:455-9.
70. Emerson DK, Limmer KK, Hall DJ, Han SH, Eckelman WC, Kane CJ et al. A receptor-targeted fluorescent radiopharmaceutical for multireporter sentinel lymph node imaging. Radiology. 2012;265:186-93.
71. Thorek DL, Abou DS, Beattie BJ, Bartlett RM, Huang R, Zanzonico PB et al. Positron lymphography: multimodal, high-resolution, dynamic mapping and resection of lymph node (s) after intradermal injection of 18F-FDG. J Nucl Med. 2012;53:1438-45.
72. Chin PT, Welling MM, Meskers SC, Valdes Olmos RA, Tanke H, van Leeuwen FW. Optical

imaging as an expansion of nuclear medicine: Cerenkov-based luminescence vs fluorescence-based luminescence. Eur J Nucl Med Mol Imaging. 2013;40:1283-91.
73. Zhou Z, Chen H, Lipowska M, Wang L, Yu Q, Yang X et al. A dual-modal magnetic nanoparticle probe for preoperative and intraoperative mapping of sentinel lymph node(s) by magnetic resonance and near infrared fluorescence imaging. J Biomater Appl. 2013;28:100-11.
74. Ma Y, Tong S, Bao G, Gao C, Dai Z. Indocyanine green loaded SPIO nanoparticles with phospholipid-PEG coating for dual-modal imaging and photothermal therapy. Biomaterials. 2013;34:7706-14.
75. van der Poel HG, Buckle T, Brouwer OR, Valdes Olmos RA, van Leeuwen FW. Intraoperative laparoscopic fluorescence guidance to the sentinel lymph node in prostate cancer patients: clinical proof of concept of an integrated functional imaging approach using a multimodal tracer. Eur Urol. 2011;60:826-33.
76. Ohnishi S, Lomnes SJ, Laurence RG, Gogbashian A, Mariani G, Frangioni JV. Organic alternatives to quantum dots for intraoperative near-infrared fluorescent sentinel lymph node mapping. Mol Imaging. 2005;4:172-81.
77. Sevick-Muraca EM, Sharma R, Rasmussen JC, Marshall MV, Wendt JA, Pham HQ et al. Imaging of lymph flow in breast cancer patients after microdose administration of a near-infrared fluorophore: feasibility study. Radiology. 2008;246:734-41.
78. Cundiff JD, Wang YZ, Espenan G, Maloney T, Camp A, Lazarus L et al. A phase I/II trial of 125I methylene blue for one-stage sentinel lymph node biopsy. Ann Surg. 2007;245:290-6.
79. Harkrider WW, Diebold AE, Maloney T, Espenan G, Wang YZ, Stafford SJ et al. An extended phase II trial of iodine-125 methylene blue for sentinel lymph node identification in women with breast cancer. J Am Coll Surg. 2013;216:599-605.
80. Riveros M, Garcia R, Cabanas R. Lymphadenography of the dorsal lymphatics of the penis. Technique and results. Cancer. 1967;20:2026-31.
81. Ahmed M, Douek M. The role of magnetic nanoparticles in the localization and treatment of breast cancer. Biomed Res Int. 2013;2013:281-230.
82. Heesakkers RA, Hovels AM, Jager GJ, van den Bosch HC, Witjes JA, Raat HP et al. MRI with a lymph-node-specific contrast agent as an alternative to CT scan and lymph-node dissection in patients with prostate cancer: a prospective multicohort study. Lancet Oncol. 2008;9:850-6.
83. Sever AR, Mills P, Jones SE, Mali W, Jones PA. Sentinel node identification using microbubbles and contrast-enhanced ultrasonography. Clin Radiology. 2012;67:687-94.
84. Jain R, Dandekar P, Patravale V. Diagnostic nanocarriers for sentinel lymph node imaging. J Control Release.2009;138:90-102.
85. Alazraki NP, Styblo T, Grant SF, Cohen C, Larsen T, Aarsvold JN. Sentinel node staging of early breast cancer using lymphoscintigraphy and the intraoperative gamma-detecting probe. Semin Nucl Med. 2000;30:56-64.
86. Buckle T, Brouwer OR, Valdes Olmos RA, van der Poel HG, van Leeuwen FW. Relationship

between intraprostatic tracer deposits and sentinel lymph node mapping in prostate cancer patients. J Nucl Med. 2012;53:1026-33.
87. Vidal-Sicart S, Brouwer OR, Matheron HM, Bing Tan I, Valdes-Olmos RA. Sentinel node identification with a portable gamma camera in a case without visualization on conventional lymphoscintigraphy and SPECT/CT. Rev Esp Med Nucl Imagen Mol. 2013;32:203-4.
88. Valdes Olmos R, Vidal-Sicart S, Giammarile F, Zaknum JJ, van Leeuwen FW, Mariani G. The GOSST concept and hybrid mixed/virtual/augmented reality environment radioguided surgery. Q J Nucl Med Mol Imaging. 2014;58:207-15.
89. Rassweiler JJ, Muller M, Fangerau M, Klein J, Goezen AS, Pereira P et al. iPad-assisted percutaneous access to the kidney using marker-based navigation: initial clinical experience. Eur Urol. 2012;61:628-31.
90. Volonte F, Buchs NC, Pugin F, Spaltenstein J, Schiltz B, Jung M et al. Augmented reality to the rescue of the minimally invasive surgeon. The usefulness of the interposition of stereoscopic images in the Da Vinci robotic console. Int J Med Robot. 2013;9:e34-8.
91. Volonte F, Pugin F, Buchs NC, Spaltenstein J, Hagen M, Ratib O et al. Console-integrated stereoscopic OsiriX 3D volume-rendered images for da Vinci colorectal robotic surgery. Surg Innov. 2013;20:158-63.
92. Vermeeren L, Klop WM, van den Brekel MW, Balm AJ, Nieweg OE, Valdes Olmos RA. Sentinel node detection in head and neck malignancies: innovations in radioguided surgery. J Oncol. 2009;2009:681746.
93. Vermeeren L, Meinhardt W, Bex A, van der Poel HG, Vogel WV, Hoefnagel CA et al. Paraaortic sentinel lymph node(s): toward optimal detection and intraoperative localization using SPECT/CT and intraoperative real-time imaging. J Nucl Med. 2010;51:376-82.
94. Wendler T, Hartl A, Lasser T, Traub J, Daghighian F, Ziegler SI et al. Towards intra-operative 3D nuclear imaging: reconstruction of 3D radioactive distributions using tracked gamma probes. Med Image Comput Comput Assist Interv. 2007;10:909-17.
95. Wendler T, Herrmann K, Schnelzer A, Lasser T, Traub J, Kutter O et al. First demonstration of 3-D lymphatic mapping in breast cancer using freehand SPECT. Eur J Nucl Med Mol Imaging. 2010;37:1452-61.
96. Heuveling DA, Karagozoglu KH, van Schie A, van Weert S, van Lingen A, de Bree R. Sentinel node biopsy using 3D lymphatic mapping by freehand SPECT in early stage oral cancer: a new technique. Clin Otolaryngol. 2012;37:89-90.
97. Rieger A, Saeckl J, Belloni B, Hein R, Okur A, Scheidhauer K et al. First Experiences with Navigated Radio-Guided Surgery Using Freehand SPECT. Case Rep Oncol. 2011;4:420-5.
98. Brouwer OR, Buckle T, Bunschoten A, Kuil J, Vahrmeijer AL, Wendler T et al. Image navigation as a means to expand the boundaries of fluorescence-guided surgery. Phys Med Biol. 2012;57:3123-36.

99. Baumhauer M, Feuerstein M, Meinzer HP, Rassweiler J. Navigation in endoscopic soft tissue surgery: perspectives and limitations. J Endourol. 2008;22:751-66.
100. Simpfendorfer T, Baumhauer M, Muller M, Gutt CN, Meinzer HP, Rassweiler JJ et al. Augmented reality visualization during laparoscopic radical prostatectomy. J Endourol. 2011;25:1841-5.